Eighth International Conference on
ADVANCES IN STEEL STRUCTURES
Lisbon, Portugal, July 22-24, 2015

MODELING OF THE NONLINEAR BEHAVIOR OF STEEL FRAMED STRUCTURES WITH SEMI-RIGID CONNECTIONS

Afsin Saritas*, Ahmet Koseoglu and Halil Firat Ozel****

* Associate Professor at Middle East Technical University
e-mail: asaritas@metu.edu.tr

** Ph.D. Student at Middle East Technical University
e-mails: ahmet.koseoglu@metu.edu.tr, firat.ozel@metu.edu.tr

Keywords: Steel framed structures; Nonlinear structural analysis; Finite element modeling; Semi-rigid connection;Hysteretic behavior

Abstract. *A mixed formulation frame finite element with internal semi-rigid connections is presented for the nonlinear analysis of steel structures. Proposed element provides accurate responses for spread of inelasticity along element length by monitoring the nonlinear responses of several cross-sections, where spread of inelasticity over each section is captured with fiber discretization. Each material point on the section considers inelastic coupling between normal stress and shear stress. The formulation of the element also considers the presence of linear or nonlinear behavior of semi-rigid connection behavior without additional nodes and degrees of freedom, thus robustness of element response is maintained. Formulation of the element can include the presence of axial and shear deformations and rotation on localized connection region. For an accurate representation of cyclic behavior of connection regions, a multi-linear model is considered that accounts for strength and stiffness degradation as well as pinching of the hysteresis curves. Nonlinear response of the proposed element is assessed by considering steel framed structures with semi-rigid connections.*

1 INTRODUCTION

Several experimental and analytical modeling of semi-rigid connections have been performed by researchers, and implementation of an accurate behavior of semi-rigid connections into structural analyses is still an ongoing research issue. One of the most cited and early study on the development and use of frame finite elements with consideration of semi-rigid connections was presented by Lui and Chen [1]. Plasticity was assumed to exist only as a lumped value at the plastic hinge location and the remaining part of the member was linear elastic; thus in order to capture yielding along beam length, beam span had to be discretized into further elements. For the moment rotation curve of the connection an exponential function was used, and in this regards the constitutive model was limited to monotonic loading. In the study of Sekulovic and Salatic [2] the effect of the connection flexibility on the behavior of the structure under static loading was examined, where a numerical model was used that takes both nonlinear behavior of the connection and geometric nonlinearity of the structure into consideration. This beam model had similar assumptions with the study by [1].

Valipour and Bradford [3] proposed a frame element that considers spread of inelasticity along element length and nonlinear semi-rigid behavior at element ends. The element has been developed based on force formulation using total secant stiffness approach. The work in the paper did not present comparisons with experimental data, and more importantly, the nonlinear response of the connection did not take into account stiffness and strength degradation and pinching effects since the researchers opted to use both a bilinear model with

kinematic hardening and alternatively the Ramberg–Osgood model. Nonlinear geometric effects were not also taken into account in the formulation.

Nguyen and Kim [4] proposed a force-based frame element that considers spread of inelasticity along element length and section depth, where the element did not include semi-rigid connections inside element response, but considered separate zero-length spring elements in order to take into account connection response in analysis at the expense of increased nodes and degrees of freedom. By the use of displacements calculated through stability analysis, nonlinear geometric effects were taken into account in element response. Verification studies in the paper only focused on monotonic responses of steel frames with semi-rigid connections. In describing connection behavior, power and exponential models were employed.

In this paper, a macro frame element model is developed for analysis of steel framed structures with spread of inelastic behavior along element length and incorporating nonlinear semi-rigid connections. The element is formulated through force-based approach and coded such that it can include any number of semi-rigid connections at arbitrary locations along an element without any need of introducing nodes and degrees of freedom. For representation of nonlinear behavior of semi-rigid connections, moment-rotation type mathematical models proposed in the literature for beam to column connections have been used for comparison of the element response via benchmark results. For a true representation of the hysteretic energy dissipation characteristic of a semi-rigid beam to column connection, a moment-rotation model incorporating pinching, damage, the possibility of residual moment capacity, degradation of stiffness is implemented. The response of developed moment-rotation model is calibrated and verified via experimental data of various semi-rigid connection types from literature. The macro element model is used in conjunction with corotational formulation for the capture of nonlinear geometric effects and to demonstrate the importance of modeling the hysteretic behavior of semi-rigid connections in the nonlinear analysis of steel framed structures.

2 FRAME ELEMENT FORMULATION WITH CONNECTORS

2.1 Derivation of element response

The element is composed of continuous element portions with discontinuities arising due to the presence of zero-length rotational springs. Kinematics of the continuous portion of the frame element follows Timoshenko Beam Theory assumptions. As part of this theory, element response is due to the presence of normal and shear stresses along element length. Nonlinear response of the continuous portion of the element is aggregated from the monitoring of the responses of several control sections along element length, and furthermore at each section, the response is assembled through fiber discretization of the section.

The formulation of the element starts with the calculation of axial force *N(x)*, bending moment *M(x)* and shear force *V(x)* from basic element forces q_1, q_2 and q_3 (Figure 1). In the absence of inter element loads, these internal forces can be simply calculated with statics knowledge as follows:

$$\mathbf{s}(x)=\begin{Bmatrix} N(x) \\ M(x) \\ V(x) \end{Bmatrix}=\begin{Bmatrix} q_1 \\ (x/L-1)q_2+(x/L)q_3 \\ -(q_2+q_3)/L \end{Bmatrix} \tag{1}$$

Above equation can be extended to the presence of distributed uniform element loads w_x and w_y applied in the axial and transverse directions, respectively, and can be written as:

$$\mathbf{s}(x) = \mathbf{b}(x)\mathbf{q} + \mathbf{s}_{\boldsymbol{p}}(x) \tag{2}$$

where **q** is the vector of basic element forces, **b***(x)* represents the force-interpolation functions and can be regarded as an equilibrium transformation between section forces **s***(x)* and basic forces **q**, and the particular solution $\mathbf{s}_{\boldsymbol{p}}(x)$ is due to uniform loads w_x and w_y, where these are all given as:

$$\mathbf{q} = \begin{Bmatrix} q_1 \\ q_2 \\ q_3 \end{Bmatrix};\ \mathbf{b}(x) = \begin{bmatrix} 1 & 0 & 0 \\ 0 & x/L-1 & x/L \\ 0 & -1/L & -1/L \end{bmatrix};\ \ \mathbf{s}_{\boldsymbol{p}}(x) = \begin{Bmatrix} w_x(L-x) \\ w_y L^2\left(x^2 - xL\right)/2 \\ w_y\left(L-2x\right)/2 \end{Bmatrix} \tag{3}$$

Principal of virtual forces necessitate the equality between virtual element end forces $\delta\mathbf{q}$ multiplied with real element deformations $\boldsymbol{v}$ to be calculated from the integration of virtual section forces $\delta\mathbf{s}$ multiplied with real section deformations **e**. Introduction of the section interpolation functions from above equations and with the fact that virtual forces are arbitrary, element end deformations **v** are calculated from the section deformations as follows

$$\mathbf{v} = \int_L \mathbf{b}^{\mathrm{T}}(x)\mathbf{e}(x)dx; \quad \text{and} \quad \mathbf{e} = \begin{pmatrix} \varepsilon_a & \kappa & \gamma \end{pmatrix}^{\mathrm{T}} \tag{4}$$

where e is the vector of section deformations.

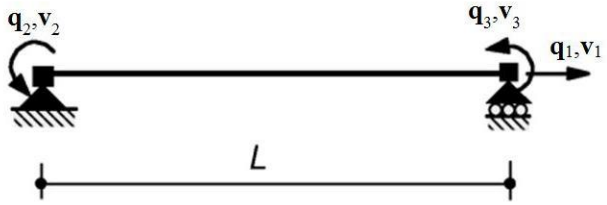

Figure 1: Basic Forces and Deformation for Beam Element

Element flexibility matrix **f** can be calculated from above equation by considering partial differentiation of **v** with respect to element end forces **q**:

$$\mathbf{f} = \frac{\partial \mathbf{v}}{\partial \mathbf{q}} = \int_L \mathbf{b}^{\mathrm{T}}(x)\mathbf{f}_s(x)\mathbf{b}(x)dx \tag{5}$$

where $\mathbf{f}_s$ is the section flexibility matrix that can be calculated from the inversion of the section stiffness matrix $\mathbf{k}_s$.

At this point in the element formulation, presence of semi-rigid connections will be introduced through the following extended version of above equation for the calculation of element end deformations:

$$\begin{aligned} &\mathbf{v} = \mathbf{v}_{\text{Frame}} + \mathbf{v}_{\text{Con}} \\ &\mathbf{v}_{\text{Frame}} = \int_L \mathbf{b}^{\mathrm{T}}(x)\mathbf{e}(x)dx; \quad \text{and } \mathbf{v}_{\text{Con}} = \sum_{i=1}^{nSC} \mathbf{b}^{\mathrm{T}}(x_i)\boldsymbol{\Delta}_{SC,i} \end{aligned} \tag{6}$$

The first integral along the length of the frame element can be numerically calculated by using a quadrature rule to capture spread of inelastic behavior and*nSC* is the total number of semi-rigid connections present along the element that is discreetly located at any distance along the length of the element; $\mathbf{\Delta}_{SC} = \left[\delta_{SC}^{axial} \quad \theta_{SC} \quad \delta_{SC}^{shear} \right]^{\mathrm{T}}$ is the vector of semi-rigid connection deformations composed of axial deformation δ_{SC}^{axial}, rotation θ_{SC} and shear sliding δ_{SC}^{shear} of a connection. Introduction of semi-rigid connections along element length in Figure 1 does not alter the force field under small deformations, thus above equalities in Equations (1) to (6) are not affected by this operation.

Element flexibility matrix is similarly discretized as follows:

$$\begin{aligned} &\mathbf{f} = \mathbf{f}_{\text{Frame}} + \mathbf{f}_{\text{Con}} \\ &\mathbf{f}_{\text{Frame}} = \int_{L} \mathbf{b}^{\mathrm{T}}(x)\mathbf{f}_{s}(x)\mathbf{b}(x)dx; \quad \text{and} \quad \mathbf{f}_{\text{Con}} = \sum_{i=1}^{nSC} \mathbf{b}^{\mathrm{T}}(x_i)\mathbf{f}_{SC,i}\mathbf{b}(x_i) \end{aligned} \tag{7}$$

It is worth to point out the variational base of the nonlinear force-based elements is proven by Saritas and Soydas [5] to be obtained through the use of three-fields Hu-Washizu functional.

The use of Gauss-quadrature or Gauss-Lobatto quadrature integration points with number of integration points *nIP* selected as 5 results in a sufficiently accurate nonlinear behavior for the continuous part [6]. In order to capture plastification along section depth, fiber discretization is employed with various integration rules, where midpoint and trapezoidal rule typically gives accurate results for attaining nonlinear response of section integrations. In this regards, it is worth to note that the frame element model presented in this paper can also successfully capture both flexure yielding in long beams and shear-yielding in short steel beams, i.e. shear-links [7]. This is achieved through the coupling of normal and shear stresses at material points along the depth of a section of the beam [8] as presented next. Instead of fiber discretization of the section, an alternative approach is to use stress resultants plasticity models to capture the interaction between section forces. Advantages and disadvantages of using such an approach over fiber discretization is presented in [9].

With regards to the nonlinear behavior of semi-rigid connections, the current study focuses on only the presence of uncoupled and nonlinear behavior for the rotational component of semi-rigid connections, thus axial and shear behaviors are obtained separately and furthermore assumed as linear elastic and infinitely strong. These assumptions provide accurate representation of the behavior of partially restrained connections for horizontal load carrying members such as beams. In the case of columns where base plate connections provide significant axial and rotation interactions, response of connections should consider axial force and bending moment coupling in nonlinear response.

2.2 Section response

Section response can be obtained by the basic assumption that plane sections before deformation remain plane after deformation along the length of the beam by the use of following section compatibility matrix $\mathbf{a}_{\mathrm{s}}$ as given

$$\boldsymbol{\varepsilon} = \begin{pmatrix} \varepsilon_{xx} \\ \gamma_{xy} \end{pmatrix} = \mathbf{a}_{\mathrm{s}}\,\mathbf{e} \tag{8}$$

where the section compatibility matrix is

$$\mathbf{a}_s = \mathbf{a}_s(y) = \begin{bmatrix} 1 & -y & 0 \\ 0 & 0 & \kappa_s \end{bmatrix} \tag{9}$$

and **e** is the section deformation vector given in Equation (4) and κ_s is the shear correction factor taken as the inverse of the form factor suggested by Charney et al.[10] for wide-flange sections:

$$\kappa_S = 1/\kappa; \quad \text{where} \quad \kappa = 0.85 + 2.32\frac{b_f t_f}{d\, t_w} \tag{10}$$

The section forces are obtained by integration of the stresses that satisfy the material constitutive relations $\boldsymbol{\sigma} = \boldsymbol{\sigma}(\boldsymbol{\varepsilon})$ according to

$$\mathbf{s} = \begin{pmatrix} N \\ M \\ V \end{pmatrix} == \int_A \underbrace{\begin{bmatrix} 1 & 0 \\ -y & 0 \\ 0 & \kappa_s \end{bmatrix}}_{\mathbf{a}_s^{\mathrm{T}}} \underbrace{\begin{pmatrix} \sigma_{xx} \\ \sigma_{xy} \end{pmatrix}}_{\boldsymbol{\sigma}} dA \tag{11}$$

The derivative of section forces from (11) with respect to the section deformations results in the section tangent stiffness matrix

$$\mathbf{k}_s = \frac{\partial \mathbf{s}}{\partial \mathbf{e}} = \int_A \mathbf{a}_s{}^{\mathrm{T}} \frac{\partial \boldsymbol{\sigma}(\boldsymbol{\varepsilon})}{\partial \mathbf{e}}\, dA = \int_A \mathbf{a}_s{}^{\mathrm{T}} \mathbf{k}_m \mathbf{a}_s\, dA \tag{12}$$

The material tangent modulus $\mathbf{k}_m$ is obtained from the stress-strain relation according to

$$\mathbf{k}_m = \frac{\partial \boldsymbol{\sigma}(\boldsymbol{\varepsilon})}{\partial \boldsymbol{\varepsilon}} \tag{13}$$

Gauss-quadrature, the midpoint or the trapezoidal rule can be used for the numerical evaluation of the integrals in (11) and (12). While Gauss-quadrature gives better results for smooth strain distributions and stress-strain relations, the midpoint rule is preferable for strain distributions and stress-strain relations with discontinuous slope.

3 SEMI-RIGID CONNECTION RESPONSE

3.1 Proposed connection model

The proposed model in this paper is a multi-linear model similar to the original work by Ibarra et al. [11]. However, in terms of theoretical development and implementation of the proposed model in this paper, the trilinear model that is already present in Fedeaslab finite element program [12] was originally considered for the theoretical development and implementation purposes in Matlab, and this trilinear model is also available in OpenSees finite element program [13] with function name *uniaxialMaterial Hysteretic*. The proposed model in this paper proposes a quadra-linear response that is extension from the trilinear response, and it is actually similar to the original model by [11] and with its implemented version in OpenSees with function name *uniaxialMaterial Pinching4*. It is worth to point out that these models were not specifically proposed for describing the behavior of semi-rigid connections, and they are mostly used in conjunction with describing localized plastic hinge

responses in reinforced concrete members. Since the proposed model in this paper is similar with those models, only a summary of the proposed model is considered to be sufficient, where differences between both models are mentioned in the following presentation and in depth discussion is available in the thesis of Koseoglu [14]. While using a multi-linear model, initial stiffness, yielding and ultimate moments can be taken from either test data or estimated through a theory as discussed in the literature review on monotonic models. The unloading stiffness in the proposed model has been taken as equal to initial stiffness which is reasonable when considering experiments.

Quadra-linear model is implemented in order to better capture pinching and residual moment capacities. Pinching can be caused by several factors in a semi-rigid connection, such as permanent deformation in yielded materials that is unrecoverable under load reversals and due to slippage. Such an action is possible for example with the permanent deformation of bolt holes from circle to ellipse shape or by permanent deformations in connecting parts (flanges, webs) between column and beam, causing separation between parts.

In the experiments in which pinching clearly governs it is also seen that stiffness degradation due to pinching is observed at a point away from zero-moment crossing as observed in the tests by [15]. This means that the stiffness of the unloading branch remains same up to a moment value in the reloading region. This moment value can be called as residual moment and used to determine the starting point of pinching. With this modification the user is allowed to define the residual moment value. Then this residual moment value is transformed to a rotation value. In other words, the rotation value of the point at which the residual moment is reached (point A' in Figure 2) is accepted as the starting point of pinching. In the modified model, this residual moment value is also used as a limiting value for the value of *maxmom* shown in Figure 2. As a result, if the stiffness of the any branch of the positive envelope curve is smaller than zero, the moment can decrease up to this residual moment value and then remains constant. This limitation is applied by calculating the rotation value of point D, *rotlim*. In the original model this limiting moment value is zero instead of residual moment and it is the point D' instead of D that is used to determine the value of *rotlim*.

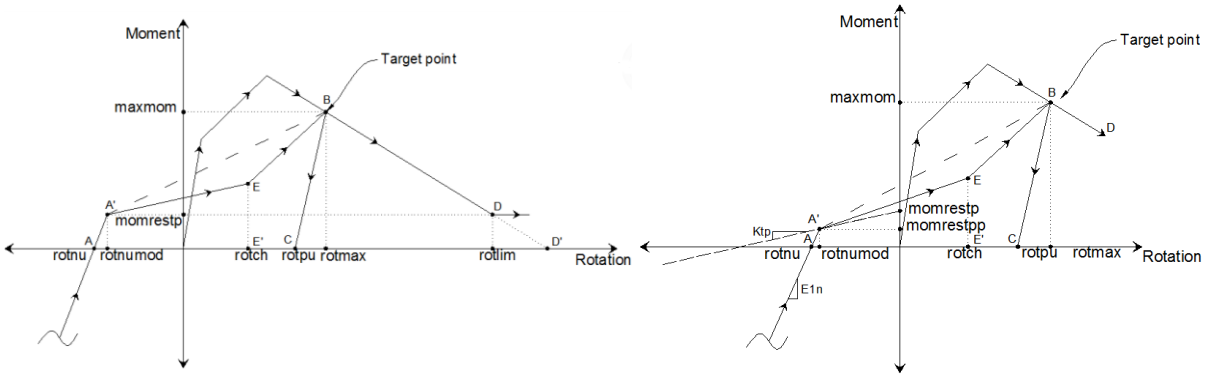

Figure 2: Behavior of the proposed quadra-linear model

Another modification introduced to the model is based on an observation that for some semi-rigid connections the residual moment may get smaller as load cycles get larger, where such an effect is absent in the model by [11]. This modification is arranged by introducing a slope value, *Ktp*, which is the slope of the line passing through a point on the moment axis. This point is selected as the point of residual moment on the moment axis (see Figure 2). This slope value *Ktp* is provided by the user. In this case a new variable called as *momrestpp* is introduced which is changing according to parameters *momrestp* and *Ktp*. It can also be

noticed that as cycles get larger the residual moment can take negative values which is reasonable when considering experimental results that are presented in the next section.

3.2 Verification of proposed model

The accuracy of the model presented above can be validated with the test results of semi-rigid connections existing in the literature. The results obtained by Abolmaali et al. [15] were first selected for this purpose. In that study two types of connections were tested namely bolted-bolted and welded-bolted double web angle connections. Bolted-bolted means angles are bolted to both beam web and column flange. Welded bolted means angles are welded to beam web and bolted to column flange. The connection between the angle and beam web is important. Because pinching mostly occurs due to enforcing of the bolts to the beam web. If the bolts have necessary strength, the circular bolt holes in the web will be oval shaped and if the angles have necessary strength the failure mode will be most probably web bearing. On the other hand when angles are welded to the beam web, due to high strength of weld, angle yielding governs the failure mode. In the study 5 bolted-bolted and 5 welded-bolted connections were used for validation. It was stated by [15] that the stiffness and strength provided by the double web angled and welded-bolted connections tested in their study provided the same stiffness and strength characteristics of moment connections.

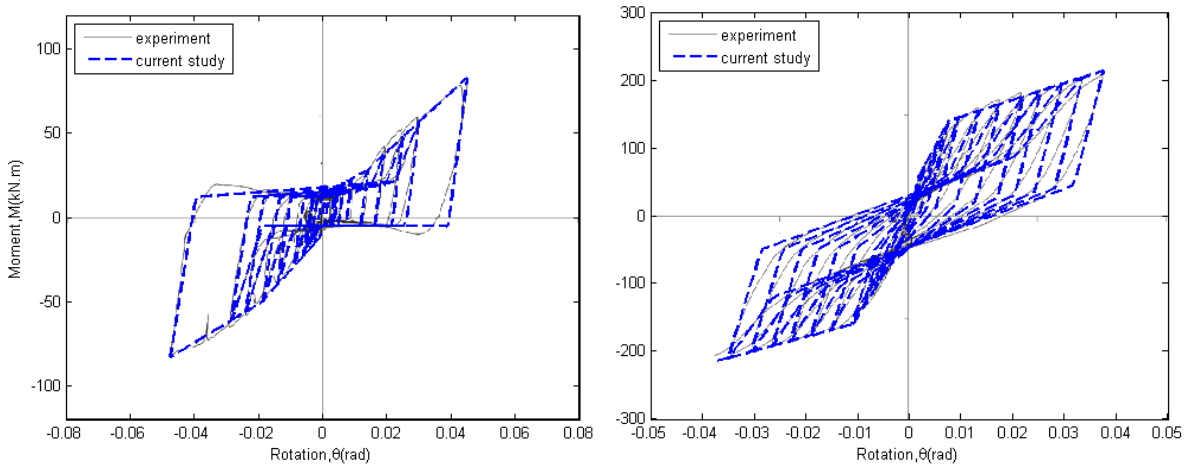

a) DW-BB-127-13-16-114-5-610 b) DW-WB-152-19-19-191-5-610

Figure 3: Comparison of proposed semi-rigid connection model for double web angle connection tests by Abolmaali et al. [15]

All of the specimens tested by [15] were successfully simulated with the proposed hysteretic connection model, but for the sake of presentation only two per connection type are presented in Figure 3, and detailed presentation of the results is available in the thesis of Koseoglu [14]. It is worth to point out that the pinching parameters of the proposed hysteretic model is obtained through calibration with experimental data and details are available in [14]; thus one can choose any level of pinching by considering the types of moment-rotation curves presented for all calibrated specimens there.

The second comparison is on the connection specimens tested by Komuro et al. [16], where two top and seat angles with double web angle (TSADWA) specimens were tested under both monotonic and cyclic loadings. It is known that TSADWA connection configuration provides a semi-rigid behavior that is closer to moment type connection and provides comparable stiffness and strength in this regards. Initial connection stiffness and the maximum moment reached in the experiment were documented by [16], and it was shown that the monotonic curve obtained by power model [17] provides close estimation of these

values with respect to experimental data. Both of TSADWA connections tested demonstrated pinching effects and residual moment capacities that are different than zero when pinching initiates. The proposed hysteretic connection model is used to demonstrate the capabilities of the model in tracing the response of the three specimens, and it is evident from Figure 4 that close fit can obtained for all specimens.

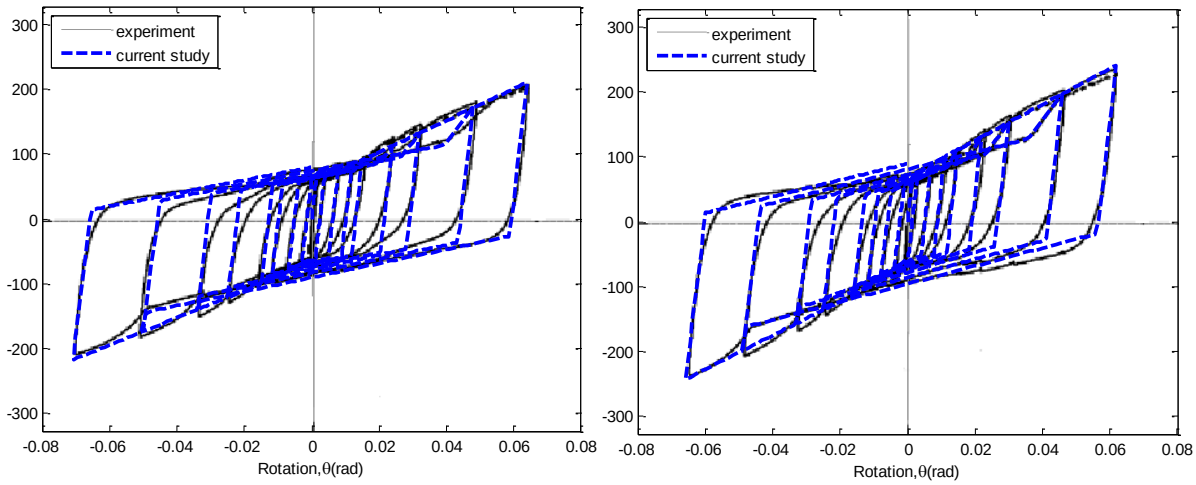

a) W18 – TSADWA connection c) W29 – TSADWA connection

Figure 4: Comparison of proposed semi-rigid connection model for top and seat angle angles with/without double web angles connection tests by Komuro et al. [16]

Last comparison is undertaken by considering the flush end plate connections tested by Bernuzzi et al. [18]. In these tests, the results of the specimens showed not only pinching effects but also strength loss, where by the way residual moment values were observed to be non-existing. The response of the proposed model vs. experimental data for two of the tested specimens is presented in Figure 5, and the proposed model is shown here to be able to follow the behavior of strength loss, as well.

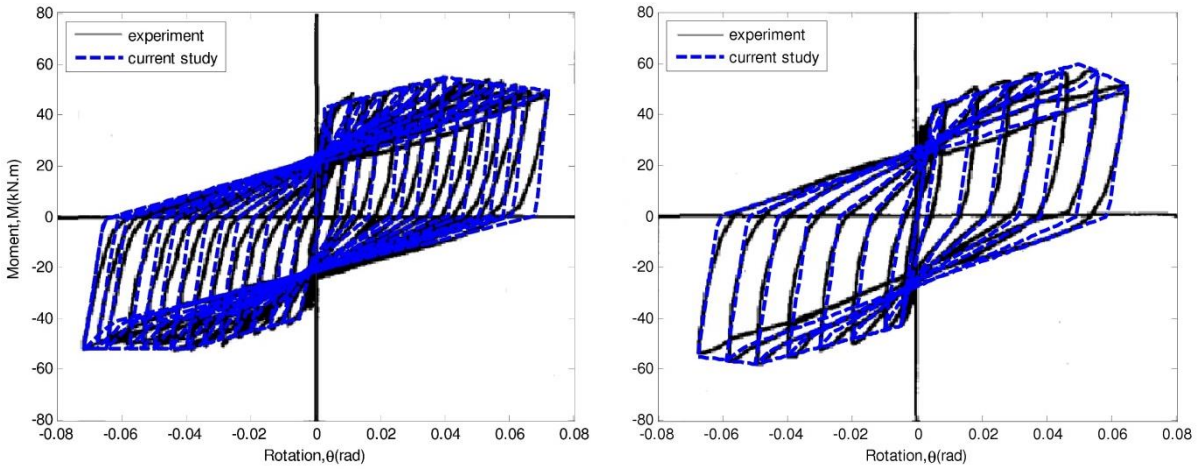

a) FPC/B connection b) FPC/D connection

Figure 5: Comparison of proposed semi-rigid connection model for flush end plate connection tests by Bernuzzi et al. [18]

4 NUMERICAL EXAMPLES

4.1 Linear elastic beam with linear end connections

Numerical validation of the response of the macro element model is first carried out under linear elastic conditions. A beam fixed at both ends is loaded along its length with a transverse distributed element load *w*. Linear elastic semi-rigid connections are introduced to the ends of the beam at fixed supports, and the stiffness of the connections k_{SR} is varied as a multiple λ of flexural rigidity *EI* of the beam divided by the length of beam *L*, i.e. $k_{SR} = \lambda EI/L$, where λ is numerically varied from infinity to zero to reflect fixed-fixed support to simply supported conditions. The beam is modeled through the use of a single macro element.

Figure 6 presents in the y-axis the moment at fixed support divided by the theoretical moment $wL^2/12$ and in the x-axis parameter λ coefficient of semi-rigid connection. On the same plot, the moment on the middle of the beam is also plotted by normalizing the value with respect to the theoretical mid-span moment for a simply supported beam under distributed load, i.e. $wL^2/8$. As the connection coefficient λ approaches theoretically to zero, the figure clearly demonstrates that simply supported beam boundary conditions are accurately reflected by the element. As the coefficient λ approaches theoretically to infinity, the moment values that should be present in a fixed-fixed beam are accurately captured. It is worth to mention that the use of connections at both ends of the element and providing a value of exactly equal to zero for λ results in stability loss for the element. In that regards, an input of zero by the user to release one end of the proposed beam from moment can be simply attained by providing a penalty value of 10^{-12} for coefficient λ to gain stability. It is worth to mention that similar analyses can also be conducted in terms of releasing the axial or shear responses for a beam, as well.

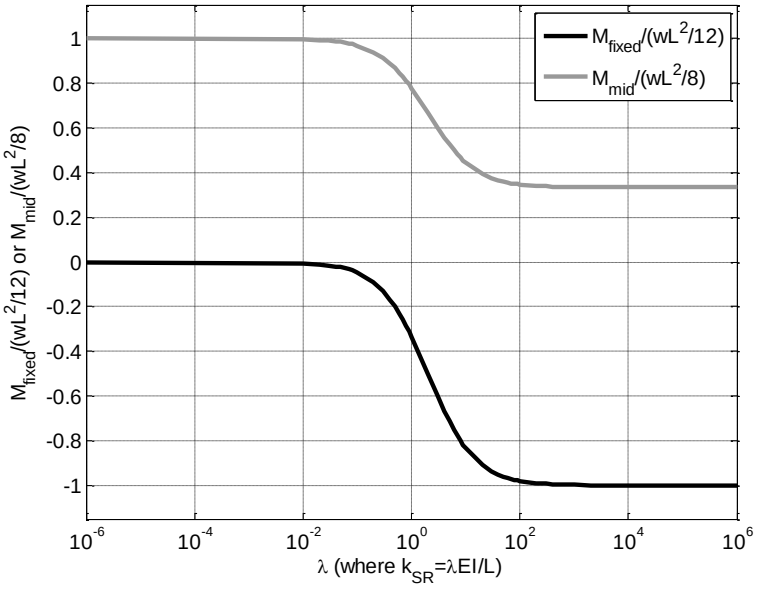

Figure 6: Moment values for varying connection stiffness to demonstrate simply supported to fixed-fixed beam boundary conditions

4.2 Rigid cantilever column with distributed linear connections

The second numerical validation example is an axially and flexurally rigid and infinitely strong cantilever column that is fixed at its base. The rigid column is introduced with n_{SR} number of semi-rigid connections distributed along its length at equal distance, where two connections are at least used to start with and they are placed at the ends of the column. While

introducing these connections, number of nodes and degrees of freedom did not change at all, i.e. the column is modeled through the use of single macro element that is proposed in this paper. The rotational stiffness of each semi-rigid connection introduced along the rigid column is assigned a rigidity of *EI* divided by a representative length L_{SR} for each connection, where $L_{SR} = L_{Col} / (n_{SR} - 1)$ along mid connections, and half of this length value at end connections. The theoretical stiffness of the response under a lateral applied force versus resulting displacement is given as $k_{Exact} = 3EI / L_{Col}^3$.

The stiffness obtained with analysis of the problem with rigid column and n_{SR} linear elastic semi-rigid connections distributed along element length is denoted as k_{SR}. Figure 7 presents the asymptotic convergence of the result of k_{SR} to k_{Exact} with increasing number of semi-rigid connections, where the connection number is increased up to 100. In order to get the result within 1% and 0.1% error, the use of 8 and 23 connectors was needed, respectively. It should be emphasized that the developed element can intake infinite number of flexible connectors in its element response without increasing the number of nodes and degrees of freedom, and this feature of the element allows reduction of data storage and increased computation time during structural analysis. While the use of so many connectors may not be needed for a single member of a steel structure, there actually exist several of such connectors in total for that structure.

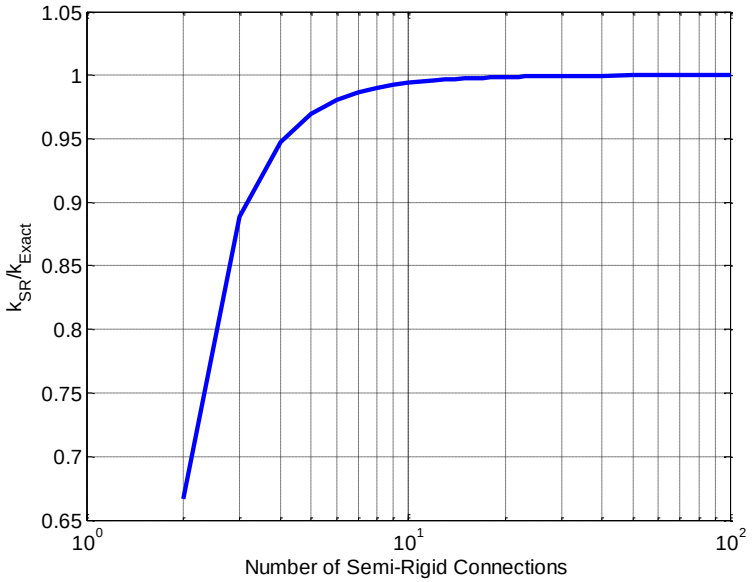

Figure 7: Increasing the number of semi-rigid connections to capture bending of a cantilever beam

4.3 Inelastic beam with nonlinear end connections

In order to present spread of plasticity along element length and presence of nonlinear action in the semi-rigid connections, a fixed-fixed supported beam with end semi-rigid connections under distributed load is considered. The beam member is analyzed by using a single element, and the response of the beam is monitored on 5 sections, where the locations are coinciding with Lobatto rule. As a result, there are two sections positioned at the ends of the beam to capture plasticity at beam's ends, and one section exactly positioned at half-span of the beam. The beam is assumed to have a rectangular cross-section with depth *d*, width *b*. On each section of the beam, 10 layers are taken to calculate the spread of plasticity along section depth, where the location of the layers is calculated from midpoint integration rule. Assuming that the material has an elastic perfectly plastic response with elasticity modulus *E*

and yield strength f_y, then the yield moment and the plastic moment capacities of the section can be calculated as $M_{y,Beam} = bd^2 f_y / 6$ and $M_{p,Beam} = 1.5M_y$, respectively. In order to demonstrate yielding and plastic hinge formation of the beam under increasing load, nonlinear response of the end semi-rigid connections are assumed to have a bilinear response with initial stiffness $k_{SR,i} = \lambda EI / L$ where $\lambda = 11$, and the yield moment capacity of the connections is assumed to be 25% of the plastic moment capacity of beam's section, i.e. $M_{y,SR} = 0.25M_{p,Beam}$, and finally the hardening stiffness of the connection is taken as 20% of its initial stiffness, i.e. $k_{SR,h} = 0.2k_{SR,i}$.

Figure 8 presents the yielding and plastic hinge formation sequence through plotting the moment at fixed support versus half-span deflection of the beam and the moment at half-span versus half-span deflection of the beam. Half-span deflection of the beam is calculated by post-processing of the calculated curvatures at monitoring sections and through the use of principle of virtual forces method. Due to the selection of the nonlinear parameters of the connections, yielding takes place in the connections first followed by the yielding of the section at half-span of the beam. Plastic moment capacity is then reached at half-span of the beam and finally the plastic moment capacities at the end sections of the beam positioned at fixed supports are reached. Moment at fixed support versus half-span deflection plot clearly demonstrates the significant change in the slope of the response due to yielding in the connection. This example clearly demonstrates the fact that the proposed element can capture plastic hinge formation along its element length, i.e. both at beam ends and along its length, in addition to the occurrence of nonlinearities in semi-rigid connections without the need for further discretization of the beam into several elements. This feature of the element provides accuracy and robustness for the nonlinear analysis of steel framed structures with partially restrained connections.

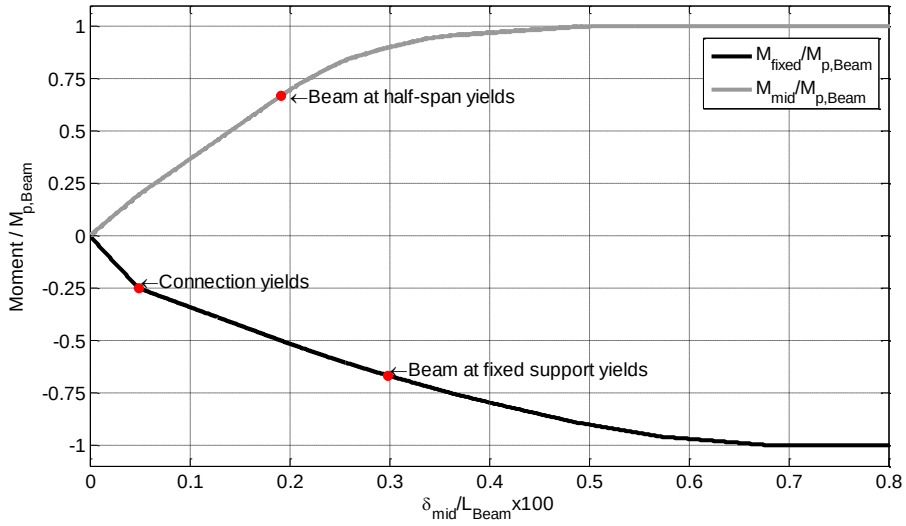

Figure 8: Yielding and plastic hinge formation for a fixed-fixed supported beam with end semi-rigid connections under distributed load

4.4 Vogel's Portal Frame

The response of the proposed element in the presence of nonlinear material and geometric effects is assessed by considering the portal frame example by Vogel [19] shown in Figure **9**. This frame was analyzed as a benchmark case by several researchers: [20], [21], and [22], where the ultimate load factor was calculated close to 1.0. It should be emphasized that this frame had rigid connections, thus those studies did not focus on modeling semi-rigid connection response as part of their research work. The deficiency of the frame with initial

imperfection and large axial load presence on the columns resulted in pronounced nonlinear geometric effect. A trilinear stress-strain behavior was assumed by [19] with a yield stress of 235 MPa and elastic modulus of 205 GPa. Perfect plasticity was assumed until 10 times the yield strain, after which strain hardening initiated with a slope of 2% of elastic modulus. The loadings shown on the frame in Figure 11 are increased proportionally with the same load factor. The analysis by [19] found the ultimate load factor as 1.017 and could not trace the post-ultimate behavior. The analysis by Teh and Clarke [21] estimated the ultimate load factor as 1.005 and provided a post-peak response, as well.

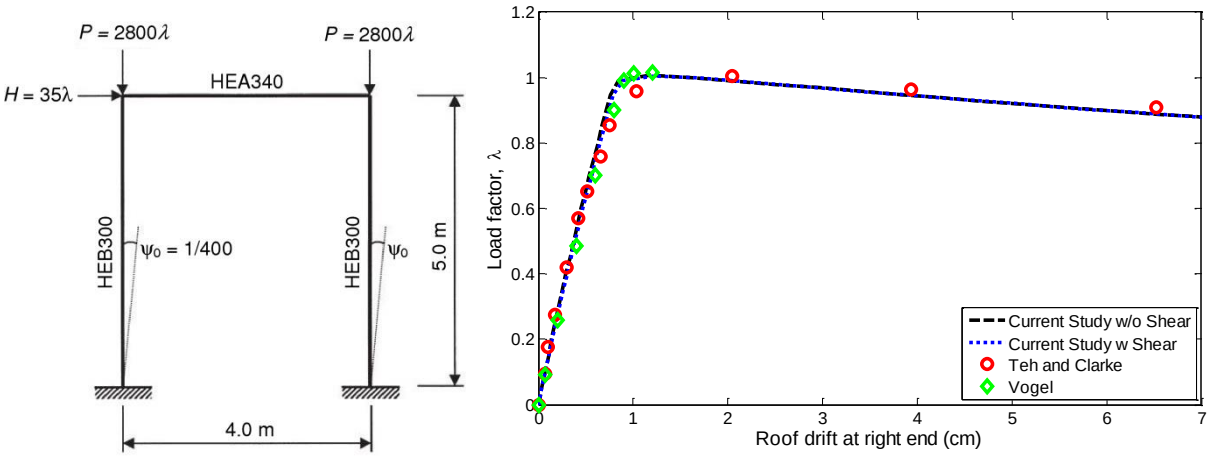

Figure 9: Portal frame and load factor vs. roof drift for [19]

In current analysis with proposed frame element with or without the presence of shear deformations, single element is used for each column and the beam, and 5 monitoring sections coinciding with Gauss rule are considered for each element. Inclusion of shear strain is once again considered only on the web and the shear correction coefficient is taken into account. Current analysis is carried out by considering a load factor incrementation and iteration strategy in order to obtain the ultimate load accurately and trace the post-peak response. It is worth to point out that only the two end monitoring sections show inelastic behavior while the middle three sections remain elastic. At each end section 4 and 8 layers are used in each flange and web, respectively, where the layer discretization is done due to trapezoidal integration rule. With this discretization, the ultimate load factor was calculated as 1.005 with and without the presence of shear deformations. A finer discretization is considered by using 10 sections where again only the two end sections show inelasticity, and 8 and 12 layers are used for each flange and web of end sections, respectively. This discretization resulted in exactly 1.000 load factor with and without the presence of shear deformations. The influence of shear is numerically negligible on ultimate load for this problem, but there is slight stiffness decrease in the presence of shear deformations. By the way, the difference in the curves obtained between current analysis and the analysis by [21] could be due to absence of modeling the residual stresses on the sections of current frame element model.

This structure was also analyzed in a recent study by Nguyen and Kim [4] and the ultimate load factor was obtained as 1.009. The same structure presented above was further analyzed by replacing the rigid beam to column connections with semi-rigid ones in the study by [4]. Connection response was modeled with the power model proposed by Kishi et al. [17], where the initial stiffness of the connection taken as 31635 kN-m/rad, ultimate moment capacity of the connection taken as 142 kN-m, and the shape parameter set to 0.98. The ultimate load factor obtained by [4] was 0.940 by the use of a spread of inelasticity model over element length and section depth and 0.924 by the use of a lumped plasticity model. The proposed

model in this paper with coarse discretization as described above resulted in 0.933 load factor with and without the presence of shear deformations, while mesh refinement resulted in 0.928 load factor with and without the presence of shear deformations.

Comparison of the load vs. displacement plots from analysis by [4] and current analysis are presented in Figure 10. It is evident that initial elastic stiffness of the structure and the ultimate load factor obtained with current study are perfectly matching the results of [4] for the case of semi-rigid connections; however, there is slight deviation of results in terms of load vs. displacement curves as seen in Figure 10. This deviation is thought to be due to the absence of residual stresses in the modeling phase of current analysis, where such a deviation was also present for the case with rigid connections in Figure 9. Exclusion of residual stresses in analysis provides slight stiffening compared to analysis with residual stresses once yielding initiates in response.

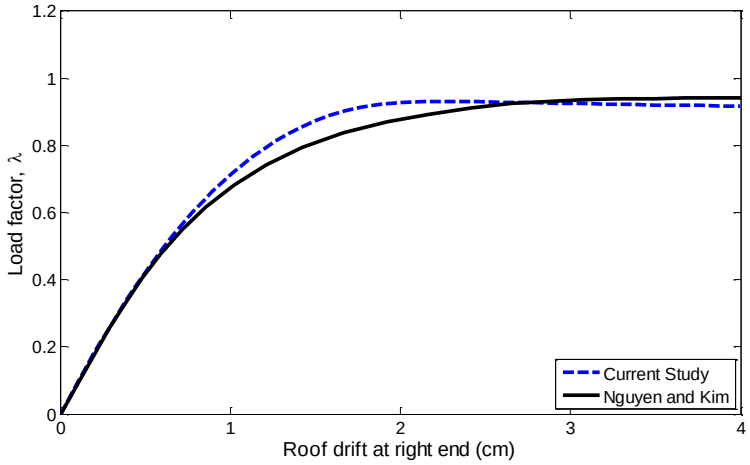

Figure 10: Load factor vs. roof drift for Vogel frame with semi-rigid connections

4.5 Stelmack's Frame

The two-story steel frame with semi-rigid beam to column connections tested by Stelmack [23] is considered as a last verification example. Boundary conditions and geometry of the members is presented in Figure 11. All members of the steel frame were made up of W5×16 beam sections with A36 steel material. Concentrated loads acting on the first story beam were first acted on and then the lateral loads with loading profile as given in Figure 11 were applied in the experiment.

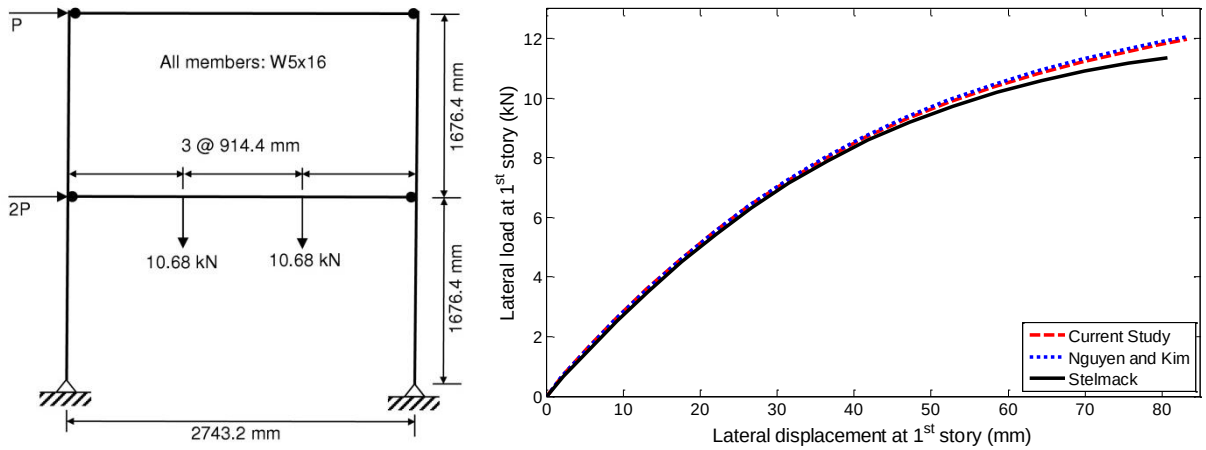

Figure 11: Lateral load vs. displacement at 1st story for two-story frame by Stelmack [23]

This experiment was considered as a benchmark verification example in the literature by Nguyen and Kim [4], as well. Moment-rotation response of the connections were presented by [23]. Response of the connections were all modeled numerically in [4] through the use of power model proposed by Kishi et al. [17], where initial stiffness of the connection was taken as 4463 kN-m/rad, ultimate moment capacity of the connection taken as 26 kN-m, and the shape parameter set to 0.87. Same model with given parameters are also considered in current study in order to provide a valid comparison not only with the experimental data by [23] but also with the numerical study undertaken by [4]. Each column is modeled through the use of single proposed frame element, first story beam is partitioned into three elements in order to apply the concentrated loads and the top story beam is modeled by considering single proposed frame element. Response of each element is obtained through a fine discretization by using 10 sections per element with Gauss-Lobatto integration rule. It is worth to point out that most of the sections remain elastic. Response of each section is obtained by fiber discretization of each section into 8 and 12 layers for each flange and web, respectively.

Comparison of the lateral load vs. displacement values at 1st story level are provided in Figure 11. It is evident that in the absence of residual stresses, the proposed frame element with localized connections clearly provide perfect match with the numerical results obtained by Nguyen and Kim [4] and close match with experimental data by Stelmack [23].

5 INFLUENCE OF HYSTERETIC CONNECTION RESPONSE

This example considers a portal frame with a single bay and one story similar to Vogel's frame in Figure 9, but this time the beam to column connections consider semi-rigidity. All columns have 3.6 m length and IPE 330 section and the beam has 6 m length and IPE 300 section; thus, ensuring strong column – weak beam design requirement. No initial imperfection is provided to the portal frame this time. Theoretical values for yield moment and plastic moment capacities of the section are calculated from elastic and plastic section moduli of IPE300 as 197 kN-m and 222 kN-m, respectively. For all columns and the beam a bilinear hysteretic steel material with f_y = 355 MPa, E = 200 GPa and E_h= 0.005E is used along element length, where each element is monitored at 5 Lobatto integration points, and at each section 4 and 8 layers are used in each flange and web, respectively, where the layer discretization is done due to midpoint integration rule. The shear response along element length is assumed to remain linear elastic. Alternatively, it is also possible to use fully coupled normal stress and shear stress response [8] to capture shear yielding behavior of short and long link members in eccentrically braced frames.

For semi-rigid connections of beams, the parameters used in the specimen shown in Figure 3.b is considered in order to incorporate hysteretic behavior in connection's cyclic response. While this connection is a double web angled and welded-bolted connection, it can be safely used for design purposes to provide the same stiffness and strength characteristics of moment connections [15]. Initial rotational stiffness for the connection is 30670 kN-m/rad; thus, the ratio between the initial stiffness of the connection with respect to the beam flexural rigidity $(EI/L)_{\text{beam}}$ is close to 11 and satisfies the partially restrained connection classification. Furthermore, plastic moment capacity of the connection for this connection was 204 kN-m, and this value in analysis is adjusted to be the same as the plastic moment capacity of the beam so that connection is as strong as the beam for the sake of analysis.

In addition to this analysis case with above selected parameters for the semi-rigid connection, an alternative analysis is also conducted, where bilinear response is assumed to be present in the semi-rigid connection instead of the proposed quadra-linear model with hysteretic behavior. The bilinear model can be considered as an approximation to the

nonlinear hardening models employed in the prior frame finite element models. It is worth to mention that the bilinear model and the nonlinear hardening models do not incorporate stiffness and strength degradation, as well as pinching behavior. For the bilinear model, the experimental backbone curve of connection response is approximated with a bilinear curve such that initial stiffness is 30670 kN-m/rad, the moment value where bilinearity starts is 150 kN-m and the hardening stiffness is set at 1650 kN-m so that the same ultimate moment is reached at the same rotation capacity. This comparison will demonstrate the importance of the modeling the hysteretic response of semi-rigid connections on the energy absorption capacity during cyclic loading without the need for conducting elaborate nonlinear structural dynamic analyses.

The beam is loaded with a 15 kN/m uniform distributed load and 50 kN additional downward acting loads are applied on top of each column. First, the gravity loads are applied, and then a cyclic displacement reversal with a magnitude of 0.5 m is imposed at the roof level. Three different analyses cases are considered in which nonlinear geometric transformations with corotational formulation was considered. The analyses cases are as follows: rigid connection model with nonlinear geometry (Rigid); bilinear semi-rigid connection model with nonlinear geometry (Semi-rigid - Bilinear); proposed semi-rigid connection model with nonlinear geometry (Semi-rigid - Hysteretic). In all analyses, spread of inelasticity along element length is taken into account. It should be emphasized that quadratic convergence rate is obtained in the presence of nonlinear geometric effects, where corotational transformation is observed to provide a stable convergence scheme in this regards. The same analyses were also conducted under linear geometric transformation, but the results were only slightly changing, thus they are not presented for comparison.

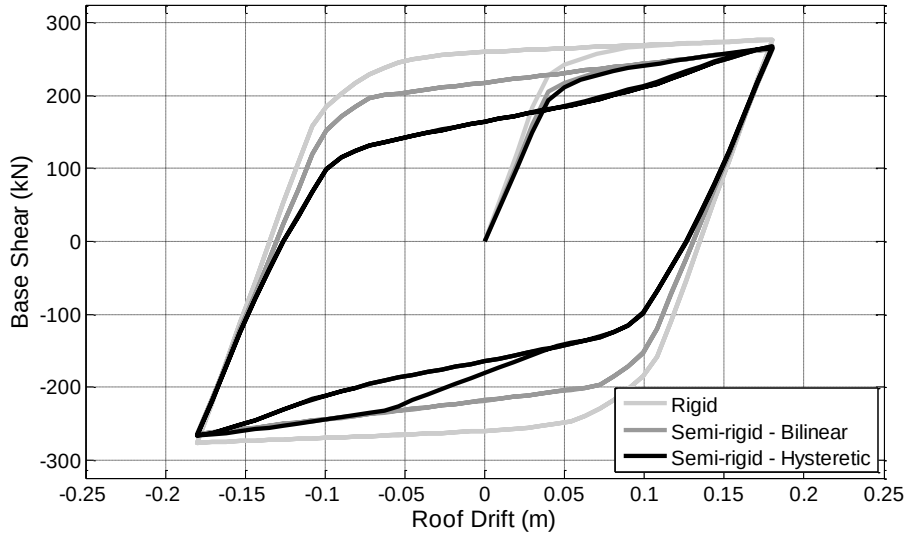

Figure 12: Effects of hysteretic behavior of semi-rigid connection and nonlinear geometry on structural response

The responses obtained from the rigid and semi-rigid cases in Figure 12 clearly demonstrate the importance of the linear and nonlinear behavior of semi-rigid connections. Moment vs. rotation response in the left semi-rigid connection and moment vs. curvature response at the left end of the beam are presented in Figure 13, where it is observed that the drop in the energy dissipation by bilinear semi-rigid (SR) connection model with respect to hysteretic connection model is compensated by increased curvature demands at both ends of the beam.

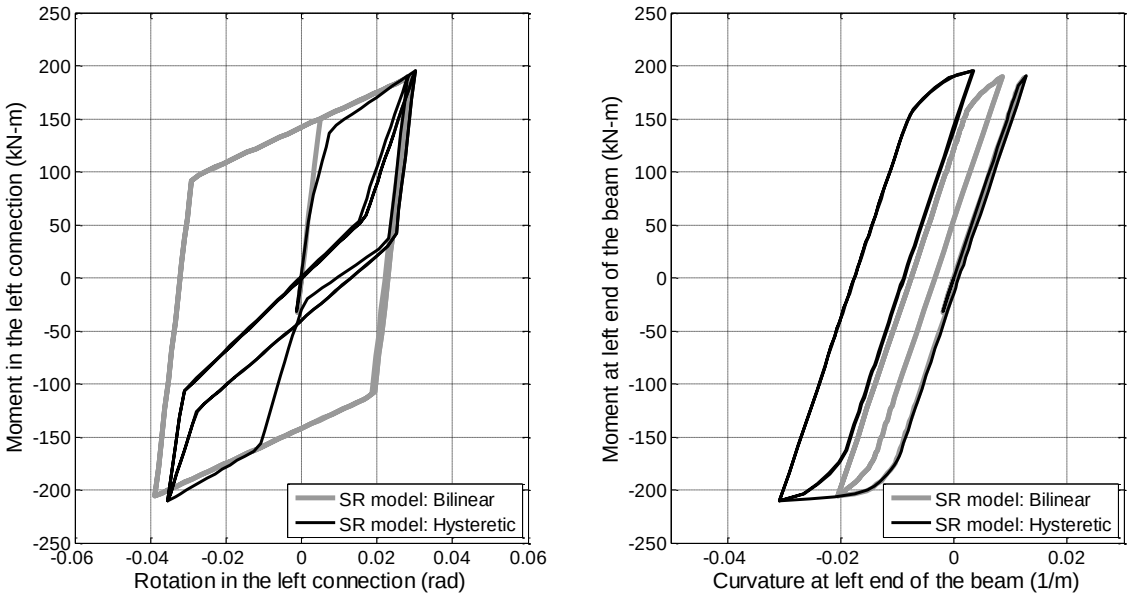

Figure 13: Response of the left connection and left end of the beam with bilinear and hysteretic semi-rigid (SR) connection models

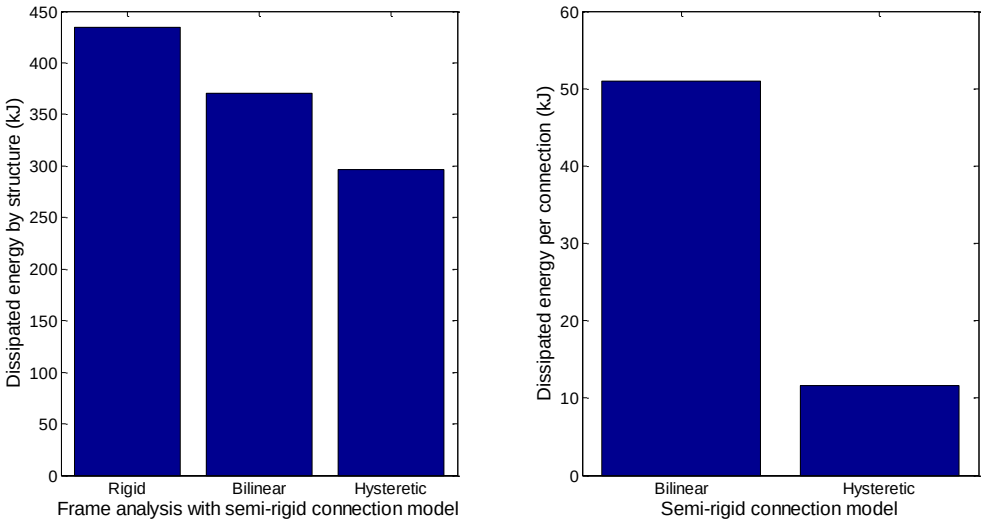

Figure 14: Dissipated energy by semi-rigid connection and structure under various modeling assumptions

Energy dissipation values in the structure and in the left semi-rigid connection are presented for different modeling strategies in Figure 14. Comparison of dissipated energy in the structure with rigid connection modeling approach and hysteretic connection modeling approach stands at 32% difference, and by the way this difference is 15% when bilinear connection model is used. Although modeling of the semi-rigid connection response with proposed hysteretic model results in 77% drop compared to the bilinear model, the influence of this modeling variation on the structure's energy dissipation remains at a much reduced but still significant level of 20% difference, since the deficiency in the dissipated energy is compensated through yielding in the ends of the beams. Although not presented here, moment vs. curvature responses of the base of the columns did not change since the amplitude of cycling was not altered in all analyses cases.

The differences in the load-deflection plots and in the energy dissipation values among the rigid model, bilinear model and proposed hysteretic model for semi-rigid connections furthermore presents the necessity of development and use of such advanced models for the description of the nonlinear response of steel structures with partially restrained connections under cyclic loadings.

6 CONCLUSION

In this paper, an accurate and robust beam element with localized semi-rigid connections is developed for the nonlinear analysis of steel structures. The element derivation bases on force formulation, and the element captures accurate behavior of spread of inelasticity along element length and section depth along beam span. Incorporation of semi-rigid connections' behavior into element response is handled without any further increase in degrees of freedom. In fact the proposed macro element can include any number of connections located along the beam; thus column tree connections can be easily analyzed by using single element per span by using the proposed element.

As part of this study, a hysteretic section model is developed for capturing the cyclic behavior of semi-rigid connections, as well. Moment rotation curves of experimental data can be closely traced due to the inclusion of residual moment capacity and pinching effects in the model. The developed section model can be easily incorporated into the macro element, and a more realistic nonlinear structural analysis can be performed.

Effect of semi-rigid connections on the initial lateral stiffness and load carrying capacity of steel structures is verified by comparison with numerical and experimental results available in the literature. Effect of pinching on the energy dissipation of the building is observed by comparing the results with the bilinear modeling approach of the semi-rigid connection. It is seen that pinching of the connections reduces the energy dissipation of a steel structure in a pronounced fashion and should be incorporated into the modeling when earthquake excitations are to be considered through a static cyclic or nonlinear time history analyses.

ACKNOWLEDGEMENT

The first and third authors thank for the support provided by Scientific and Technological Research Council of Turkey (TUBITAK) under Project No: 113M223.

REFERENCES

[1] Lui, E.M. and W.F. Chen, *Analysis and behaviour of flexibly-jointed frames.* Engineering Structures, 1986. 8(2): p. 107-118.

[2] Sekulovic, M. and R. Salatic, *Nonlinear analysis of frames with flexible connections.* Computers and Structures, 2001. 79(11): p. 1097-1107.

[3] Valipour, H.R. and M. Bradford, *An efficient compound-element for potential progressive collapse analysis of steel frames with semi-rigid connections.* Finite Elements in Analysis and Design, 2012. 60: p. 35-48.

[4] Nguyen, P. and S. Kim, *An advanced analysis method for three-dimensional steel frames with semi-rigid connections.* Finite Elements in Analysis and Design, 2014. 80: p. 23-32.

[5] Saritas, A. and O. Soydas, *Variational base and solution strategies for non-linear force-based beam finite elements.* International Journal of Non-Linear Mechanics, 2012. 47(3): p. 54-64.

[6] Taylor, R.L., F.C. Filippou, A. Saritas, and F. Auricchio, *A mixed finite element method for beam and frame problems.* Computational Mechanics, 2003. 31(1-2 SPEC.): p. 192-203.

[7] Saritas, A. and F.C. Filippou, *Frame element for metallic shear-yielding members under cyclic loading.* Journal of Structural Engineering, 2009. 135(9): p. 1115-1123.

[8] Saritas, A. and F.C. Filippou, *Inelastic axial-flexure-shear coupling in a mixed formulation beam finite element.* International Journal of Non-Linear Mechanics, 2009. 44(8): p. 913-922.

[9] Saritas, A., *Stress resultants plasticity with general closest point projection.* Mechanics Research Communications, 2011. 38(2): p. 126-130.

[10] Charney, F.A., H. Iyer, and P.W. Spears, *Computation of major axis shear deformations in wide flange steel girders and columns.* Journal of Constructional Steel Research, 2005. 61: p. 1525–1558.

[11] Ibarra, L.F., R.A. Medina, and H. Krawinkler, *Hysteretic models that incorporate strength and stiffness deterioration.* Earthquake Engineering and Structural Dynamics, 2005. 34: p. 1489-1511.

[12] Filippou, F.C., *FEDEASLab Finite Elements in Design, Evaluation and Analysis of Structures*, 2004.

[13] McKenna, F., G.L. Fenves, and F.C. Filippou, *OpenSees, Open System for Earthquake Engineering Simulation*, 1999: Berkeley.

[14] Köseoğlu, A., *A finite element model for partially restrained steel beam to column connections*, in *Civil Engineering*2013, Middle East Technical University: Ankara.

[15] Abolmaali, A., A.R. Kukreti, and H. Razavi, *Hysteresis behavior of semi-rigid double web angle steel connections.* Journal of Constructional Steel Research, 2003. 59(8): p. 1057-1082.

[16] Komuro, M., N. Kishi, and R. Hasan, *Quasi-static loading tests on moment-rotation behavior of top- and seat-angle connections*, in *Conference on Behavior of Steel Structures in Seismic Areas*2003: Naples, Italy.

[17] Kishi, N., W.F. Chen, R. Hasan, and K.G. Matsuoka, *Design aid of semi-rigid connections for frame analysis.* Engineering Journal, AISC, 1993(3rd Quarter): p. 90-107.

[18] Bernuzzi, C., R. Zandonini, and P. Zanon, *Experimental analysis and modelling of semi-rigid steel joints under cyclic reversal loading.* Journal of Constructional Steel Research, 1996. 38(2): p. 95-123.

[19] Vogel, U., *Calibrating frames.* Stahlbau, 1985. 54: p. 295–301.

[20] Ziemian, R.D. *A verification study for methods of second-order inelastic analysis*. in *Proc., 1992 SSRC Annu. Tech. Session: Earthquake Stability Problems in Eastern North America*. 1992.

[21] Teh, L.H. and M.J. Clarke, *Plastic-zone analysis of 3d steel frames using beam elements.* Journal of Structural Engineering, 1999. 125: p. 1328-1337.

[22] Iu, C.K. and M.A. Bradford, *Higher-order non-linear analysis of steel structures Part II: Refined plastic hinge formulation.* Advanced Steel Construction, 2012. 8(2): p. 183-198.

[23] Stelmack, T.W., *Analytical and Experimental Response of Flexibly-Connected Steel Frames*, in *Department of Civil, Environmental and Architectural Engineering*1982, University of Colorado at Boulder.